Accurate extreme-value-based frequency response bounding for structures with a small number of highly random parameters

Article (Accepted Version)

ACCURATE EXTREME-VALUE-BASED FREQUENCY RESPONSE BOUNDING FOR STRUCTURES WITH A SMALL NUMBER OF HIGHLY RANDOM PARAMETERS

by

J.F. Dunne* and T. Cheepsomsong

Department of Engineering and Design
The School of Engineering and Informatics
The University of Sussex, Falmer, Brighton, BN1 9QT, UK.

* Corresponding author

ABSTRACT

A modified extreme-value-based methodology is discussed for computing statistical bounds associated with the magnitude of the frequency response of a specified number of structures with high levels of random parameter uncertainty. The methodology, intended for small numbers of uncertain parameters, is capable of constructing accurate statistical bounds in terms of quantiles associated with the extreme value distribution. Quantiles can be constructed for an ensemble of structural responses across the entire frequency range without using Monte Carlo Simulation. To test the methodology, statistical bounds for the energy of an L-shaped structure with low and high levels of uniformly-distributed length and thickness variability are obtained: i) via direct integration using an ANSYS Finite Element model, and ii) via Statistical Energy Analysis (SEA). Comparisons are shown with bounds obtained using Monte Carlo simulation. The merit of direct integration for computing bounds associated with the responses of an ensemble of structures with high levels of random parameter uncertainty is demonstrated by its simplicity, high accuracy, and absence of statistical scatter.

Keywords: ensemble analytical response bounds random parameters

11 main-section pages (double-spaced) 32 references Figures 1 – 9 1 appendix

1. INTRODUCTION

Accurate computation of an upper bound on the frequency response of a specified number of uncertain structures is important in automotive and aerospace design. Uncertainty can arise from variability in materials, manufacture, and assembly, and can be modelled deterministically [1-3], in a fuzzy sense [4-5], or statistically [6-13]. Focusing on statistical bound prediction, complexity depends on the defined frequency range, whether low, mid, or high frequency. Approximate low frequency methods apply to structures responding in relatively few modes such as the Stochastic FEM [14], or the First and Second Order Reliability Methods [15–18]. Monte Carlo simulation is a more practical approach at low frequency but obtaining low probabilities needed to construct a statistical bound is often impractical in its raw form. Importance or Line Sampling [19-20] can speed-up the process (as available in the software COSSAN [21]) but accuracy is not guaranteed. High frequency methods apply to structures with vibration wavelengths much shorter than component dimensions for which SEA is most successful [22–26]. SEA takes no account of differing levels of parameter variability because randomness is assumed to be sufficiently high for knowledge of variability not to be needed. Mid-frequency responses occur when parts of a structure have wavelengths longer than component dimensions, whereas others have shorter wavelengths. A hybrid Mid-frequency method has been developed to couple the FEM and SEA [11], and further advanced in [27] to include an additional discrete system with explicitly uncertain parameters.

High levels of dominant parameter variability can however occur in practice where coefficients of variation (COV) can approach 25%. When highly random parameters dominate, SEA is not generally appropriate for bounding. Monte Carlo simulation by contrast (in addition to being expensive) is prone to statistical scatter when used for constructing statistical bounds using low exceedance probabilities. A challenge then for built-up structures with high levels of random parameter uncertainty is accurate computation of

statistical bounds across the frequency range with low probabilities of exceedance. Extreme-Value-based FRF bounding of randomly uncertain structures was first proposed in [12] and shown in [28] to apply across the entire frequency range. But a limitation in its original form is that some Monte Carlo simulation is needed. This limitation can be overcome by making a lognormal assumption [29] resulting in a very simple scatter-free bound prediction method for built-up structures not involving any Monte Carlo simulation but intended only for use with a small number of parameters. Accurate prediction involving a small number of highly random parameters is still of practical value. The objective of this paper is to assess, by comparison with Monte Carlo simulation, the accuracy of a lognormal modification to EV-based FRF bounding of a structure with a single highly random parameter. Two approaches to the modification are examined: i) via direct Integration, and ii) using a SEA model to assess the potential for highly-efficient bounding, even if SEA is used for a purpose for which it was never intended.

2. BOUNDING THE RESPONSE OF A STRUCTURE WITH RANDOM PARAMETERS

Consider an externally-forced structure in which there are a small number of random physical parameters such as one or more random plate thicknesses or lengths. These random parameters can be designated by vector $\mathbf{X} = [X_1 \;\; X_2 \;\; ... \;\; X_N]^{\mathrm{T}}$ with an assumed joint probability density function $f(\mathbf{X})$. From a modelling viewpoint, this random variability will generally be distributed throughout the structural dynamic model. For example, in a linear model, a single random parameter will distribute randomness throughout the system matrices, particularly the mass and stiffness. Assuming the structure has a steady-state dynamic response resulting from point-force harmonic excitation of known amplitude and frequency, at a particular location, the magnitude of all frequency response functions (FRFs) will be uncertain at all locations. In fact, an FRF magnitude (such as a receptance or a mobility) will in general be a random quantity at all frequencies. The challenge, given a particular number of structures, with known physical parameter randomness, is to construct

a statistical upper bound on the absolute magnitudes of the ensemble of frequency response functions. Extreme value statistics have provided a fruitful method to define such a bound [12][28]. The contribution in this paper is to provide an accurate analytical way of constructing this bound.

In the original form of extreme value bounding method [12], a small sample of FRFs obtained from Monte Carlo simulation was used to repeatedly fit (at discrete frequencies) inverted Type I asymptotic threshold exceedance models [30]. The 'bound' then predicted, gives the response amplitude level that will be exceeded on average once by the specified number of (random) structures in the sample. Here, similar notions are used at a particular frequency, to bound the magnitude of the response for *n* uncertain structures using an extreme value distribution for a finite sample rather than assuming an asymptotic model (with an infinite sample size) as in [12].

The extreme value distribution of interest is associated with random variable $M_n = \max\{Y_1, Y_2, \dots, Y_n\}$, where Y_i are assumed to be independent and identically distributed. Variable Y_i represents the absolute magnitude for any structural dynamic response of interest, such as displacement, velocity, or the spatially-averaged energy. The distribution of the maximum response M_n (in *n* realisations) is given as:

$$\Pr\{M_n \leq y\} = F_n(y) = F(y)^n \tag{1}$$

A bound of the magnitude of the response for *n* uncertain structures is defined in terms of the 100p%-quantile Z_p associated with the distribution of M_n which satisfies the equation $\Pr(M_n \leq Z_p) = p$ [31]. The bound Z_p thus satisfies the equation:

$$F_n(Z_p) = p \tag{2}$$

The challenge in general is to obtain an analytical expression for the distribution $F(y)$.

2.1 Extreme Response bounding based on a lognormal assumption for the FRF

For an assumed set of properties for the highly random parameters, the distribution $F(y)$ associated with an FRF magnitude, is generally not possible to construct analytically. There

is however good evidence to suggest that for high levels of randomness, the probability density function associated with spatially-averaged energies for example, is lognormal [29]. In fact, there is good reason to assume that the distribution for any type of absolute magnitude of response is approximately lognormal, including displacement, velocity or energy. A lognormal variable can be defined by considering a transformation to a standard normal variable $U = (\log_e(Y) - \mu)/\sigma$ [31]. Variable Y under such a transformation has a lognormal distribution with a 2-parameter density function:

$$f_Y(y) = \frac{1}{y\sigma\sqrt{2\pi}} \exp\left(-\frac{[\log_e(y) - \mu]^2}{2\sigma^2}\right), \qquad y > 0 \tag{3}$$

where parameters μ and σ are the mean and standard deviation of $\log_e(Y)$. From the moment function $E(Y^r) = \exp(r\mu + \frac{1}{2}r^2\sigma^2)$ [31] (for the r^{th} moment of Y), explicit expressions for the parameters in equation (3) can be obtained in terms of the mean μ_Y and variance σ_Y^2 of the lognormal variable Y in the form:

$$\mu = \log_e\left(\frac{\mu_Y}{\sqrt{1 + \frac{\sigma_Y^2}{\mu_Y^2}}}\right) \tag{4}$$

and

$$\sigma^2 = \log_e\left(1 + \frac{\sigma_Y^2}{\mu_Y^2}\right) \tag{5}$$

By making the lognormal assumption for the absolute response magnitudes of interest for each realised structure, a set of identical, independent random variables Y_i then exists, each with a lognormal density given by equation (3). Several routes are available to analytically calculate the mean and variance of the absolute magnitude of the frequency response amplitude of a structure with one or more random physical parameters. When these calculated moments are deemed to correspond to a lognormal variable, they can then be assumed to correspond to the moments μ_Y and σ_Y^2 to be used in equations (4) and (5) to

obtain the distribution parameters. This is effectively a lognormal density fit using equation (3) which can then be used in equation (1) to construct the quantile Z_p satisfying equation (2), to provide a statistical bound of the magnitude of the response of *n* independent (random) structures. The routes to calculate μ_Y and σ_Y^2 include Direct Integration (as applied shortly) and Statistical Energy Analysis (SEA), which requires construction of a SEA model for a particular structure. The details of SEA model predictions for an appropriate structure, collected together from various published sources, are shown in the appendix. First, the approach via integration is explained for random parameters with any type of distribution.

2.2 Computing the mean and variance of the FRF amplitude via Integration

Direct integration, involves a deterministic calculation using a function that is the absolute magnitude of a characteristic of the response at some location on the structure, resulting from harmonic point-force excitation being applied, in general, at some different location. This function describes the magnitude of the dynamic response property as a function of a deterministic variation in the component values of a selected (random) parameter vector from their nominal component values. The response property of interest could be displacement, velocity, or energy, and would typically be obtained from an appropriate frequency response function. For example, when a single parameter, such as a length or thickness dimension, is varied by a small percentage from its nominal value, a deterministic response relationship exists at each excitation frequency. This is generally a strongly nonlinear function of the form $y = g(x)$, where *x* is the designated parameter value, and the variable y is the magnitude of the characteristic of the structural response. The function $y = g(x)$ would typically be obtained using the Finite Element method involving a single deterministic calculation (i.e. not using Monte Carlo simulation, therefore involving no statistical scatter). To construct $y = g(x)$ at all frequencies, and at sufficient discrete values

of *x*, substantial computing may be needed. However once this deterministic function has been generated, the bound can be constructed for any level of parameter uncertainty.

For a multiple set of randomly uncertain parameters the magnitude of the characteristic of the response $y = g(\mathbf{x})$ is a function of the random parameter vector $\mathbf{X} = [X_1 \ X_2 \ \ldots \ X_N]^{\mathrm{T}}$. Assuming the joint pdf $f(\mathbf{X})$ is known, the mean and variance can be obtained from:

$$\mu_Y = E(y) = E(g(\mathbf{X})) = \int_{\infty}^{\infty} \cdots \int_{\infty}^{\infty} g(\mathbf{x}) f(\mathbf{x}) d\mathbf{x} \tag{6}$$

and

$$\sigma_Y^2 = E(g(\mathbf{X})^2) - E^2(g(\mathbf{X})) \tag{7}$$

where $E(g(\mathbf{X})^2)$ is obtained from:

$$E(g(\mathbf{X})^2) = \int_{\infty}^{\infty} \cdots \int_{\infty}^{\infty} g(\mathbf{x})^2 f(\mathbf{x}) d\mathbf{x} \tag{8}$$

The joint pdf $f(\mathbf{x})$ can be a subject of much conjecture. But it is expected that structures fabricated using plate or strip, formed by hot or cold rolling, will exhibit significant thickness variability. And structures just a few metres in length, are likely to have significant spatial correlation since rolling mill strip speeds can approach 10 m/s.

2.3 Direct Integration (DI) involving a single uniformly-distributed parameter

For a structure with a single random parameter, with response function $y = g(x)$, calculation of the mean μ_Y and variance σ_Y^2 needed for equations (4) and (5) is much simplified by direct integration (DI) assuming a uniform-distribution for the random parameter having mean μ_x and standard deviation σ_x. The pdf for variable X is then:

$$f(x) = \frac{1}{2a} \qquad \mu_X - a <= x <= \mu_X + a \tag{9}$$

The term a in equation (9) is directly related to the Coefficient of Variation (COV), namely $a = \sqrt{3}\mu_X \mathrm{COV}$, where $\mathrm{COV}(X) = \sigma_X / \mu_X$, therefore when the mean value μ_X is fixed, for

different COV, the value a must change. The integrals in equations (6) and (8), therefore specialise to functions of a as follows:

$$\mu_Y(a) = E(g(X)) = \int_{\mu_x-a}^{\mu_x+a} g(x)\, f(x)dx \tag{10}$$

and

$$E(g(X)^2) = \int_{\mu_x-a}^{\mu_x+a} g(x)^2\, f(x)dx \tag{11}$$

When $g(x)$ is a highly nonlinear function (as is generally the case), and the random parameter mean μ_X is fixed at the nominal value, incremental integration offers an efficient way to use equations (10) and (11) to obtain the response mean μ_Y and variance σ_Y^2 for an arbitrarily large discrete range of values of $\mathrm{COV}(X) = \sigma_X/\mu_X$. This exploits the fact that for a uniform distribution, $\sigma_X = \frac{a}{\sqrt{3}}$; and for specific values of fixed mean μ_X, the integration limit parameter $a = \sqrt{3}\sigma_X$. Thus an efficient way to use equations (10) and (11) for a range of discrete COV values, is to target the integration limits on the maximum value of COV allowing μ_Y and σ_Y^2 be obtained for all intermediate COV values in two respective incremental integrations as follows:

$$\mu_Y(a) = \int_{\mu_x-a}^{\mu_x+a} g(x)\, f(x)dx = \frac{1}{2a}\int_{\mu_x-a}^{\mu_x+a} g(x)dx = \frac{a'}{a}\,\mu_y(a') + \frac{1}{2a}\left[\int_{a'}^{a} g(x)dx + \int_{-a}^{-a'} g(x)dx\right] \tag{12}$$

and

$$E(g(X)^2) = \int_{\mu_x-a}^{\mu_x+a} g(x)^2\, f(x)dx = \frac{1}{2a}\int_{\mu_x-a}^{\mu_x+a} g(x)^2 dx = \frac{a'}{a}\,E_{g^2}(a') + \frac{1}{2a}\left[\int_{a'}^{a} g(x)^2 dx + \int_{-a}^{-a'} g(x)^2 dx\right] \tag{13}$$

The computational efficiency of the DI approach is best realised for low exceedance probabilities where the computational cost of Monte Carlo simulation is highest. Testing of

EV predictions using DI on a built-up structure is now explained, along with the use of SEA to obtain the mean and standard deviation instead of by integration.

3. A TEST ON AN L-SHAPED PLATE STRUCTURE

Constructing a bound in the form of quantile Z_p satisfying equation (2), using both Direct Integration of Section-2, and via a published SEA model (shown in the appendix), is now applied to a test problem and compared with Monte Carlo simulation using an ANSYS FE model. The test structure involves a pair of plates connected to form a coupled L-shaped structure with a 90° joint as shown in Figure 1. Two single parameters are varied separately, i.e. the plate length, and thickness parameters. Plate-1 is nominally 400 mm by 300 mm, and Plate-2 is nominally 300 mm by 200 mm. Both plates have a nominal thickness of 1 mm, density 7900 kg/m^3, Young's modulus = 200 x 10^9 N/m^2, Poisson's ratio of 0.3, and an assumed loss factor of 0.01. A single point (harmonic) force is applied on Plate 1 at coordinates x = 0.14 m and z = 0.12 m. Plate 1 is simply-supported at the edges i.e. at z = 0 m and z = 0.3 m.

Figure 2 shows an example of the ANSYS generated response function $y = g(x)$ (discussed in Section 2) with a single point load on Plate 1. This shows at frequencies 5005 Hz and 10000 Hz, the variation in the response energy for Plates 1 and 2, as a function of the plate thickness. When COV = 20% and the nominal plate thickness =1 mm for example, the value for parameter $a = 0.346\,\mathrm{mm}$ in equations (12) and (13), where a total of 150 parameter subintervals are used. The FE model is used to calculate the displacements from 10 Hz to 10000 Hz in 201 intervals. Bending, longitudinal, and shear waves are considered, where displacements for Plates 1 and 2 are then transformed into energy.

Figure 3 demonstrates correct implementation of the SEA model [24] in obtaining the mean and variance for use in equations (4) and (5). Figure 3a shows SEA model predictions of the mean and relative variance of the energy of Plates 1 and 2 versus frequency. This model corresponds to a pair of obliquely-coupled plates, with an included angle of 120º, and a

harmonically-varying point load on Plate 1. These SEA predictions are in complete agreement with the results published in [24] shown again in figure 3b.

Figure 4 and figure 5 respectively show the mean and standard deviation of the energy of Plate 1 as a function of frequency, for the L-shaped plate structure with uniformly distributed plate dimension variation, and for COV values in the plate dimension of 1%, 5%, 10%, 20%, and 30%. The response energy mean and standard deviation are obtained via Direct Integration, SEA, and Monte Carlo simulation. Figures 6 and 7 show similar information for thickness variation. For dimension variations of Plate 2, although not shown, the predicted mean energy and standard deviation via Direct Integration and SEA are both in very good agreement.

The mean μ_y and variance σ_y^2 obtained via Direct Integration (DI) and SEA, plus equations (4) and (5), and the lognormal assumption, are now used to bound the response in terms of the 50%-quantile $Z_{0.5}$ satisfying equation (2). Figure 8 shows the predicted bound expressed as the 50%-quantile for the energy response for Plate-1 with uniformly distributed dimension variation in Plates 1 and 2 for COV values of 1%, 5%, 10%, 20%, and 30%. The ensemble of realisations is obtained from ANSYS-based Monte Carlo simulations (for 100 structures). Figure 9 also shows the predicted 50%-quantile for the energy response for Plate-1 with uniformly distributed thickness variation in Plates 1 and 2 with COV values of 1%, 5%, 10%, 15%, and 20%.

Discussion of Results

First considering the response function, Figure 2 clearly shows (at two frequencies) that the response $y = g(x)$ is a very nonlinear function of the parameter variation. Figures 4 to 7 compared with Monte Carlo simulation show that direct integration produces almost identical mean and variance as Monte Carlo simulation. The corresponding SEA model predictions for Plate-1 are generally very good for low-level randomness but as expected, are not accurate at all frequencies. The SEA model predictions are significantly in error for high-

level randomness, especially for thickness variability. This is not surprising because SEA is being used in a way never intended i.e. for small numbers of random parameters. The accuracy of the predicted moments via direct integration translates into excellent 50%-quantiles as shown in Figures 8 and 9 respectively. This also implicitly confirms that the lognormal assumption is very good.

Predictions of a statistical bound across the frequency range becomes difficult by Monte Carlo simulation when the exceedance probability is significantly reduced and the target number of structures is significantly increased. Since Direct Integration involves deterministic calculations, it can therefore be used to obtain quantiles involving the tails of the extreme value distribution where Monte Carlo simulation becomes excessively expensive owing to the very large number of simulation runs needed. For a larger number of random parameters, generation of the multidimensional response function $y = g(\mathbf{x})$ needed in equations (6) and (8), will become much more demanding, and so too will the Direct Integration itself. This will justify adoption of alternatives such as Monte Carlo integration, which has $1/\sqrt{m}$ convergence where *m* is the number of samples, regardless of the number of variables involved.

4. CONCLUSIONS

A modified methodology is discussed for computing statistical bounds associated with the magnitude of frequency responses for a specified number of structures with high levels of random parameter uncertainty. The methodology, which is intended for a small numbers of uncertain parameters, exploits a lognormal assumption to enable accurate statistical bounds to be constructed in the form of quantiles associated with an extreme value distribution. This is achieved across the entire frequency range without using Monte Carlo Simulation. Testing involves an L-shaped structure with low and high levels of uniformly-distributed length and thickness variability. The lognormal density needed to construct the extreme value distribution is fitted using calculated response means and variances obtained by direct

integration (using an ANSYS Finite Element model), and via Statistical Energy Analysis (SEA). Comparisons for are also made with Monte Carlo simulation. The paper shows that direct integration gives high accuracy statistical bounds in a very simple way without statistical scatter.

APPENDIX

STATISTICAL ENERGY ANALYSIS MODEL FOR AN L-SHAPED PLATE

An alternative way to approximate an extreme-value-based bound, particularly at high frequency via equations (1), is by using Statistical Energy Analysis (SEA) to obtain the mean and variance in equation (3). Because the SEA theory for an L-shaped plate is spread over a number of sources i.e. [6][22][24] and [32], this appendix serves to bring the results together. SEA involves splitting the system into subsystems enabling the mean and variance to be obtained with computational efficiency. No assumptions are made about the distribution of the uncertain parameters but it is necessary to assume that the response statistics are constant. This means that the SEA predicted response bounds will be independent of the level of parameter uncertainty. To adapt the available theory to an L-shaped structure this can be treated as a special case of the oblique junction [6] shown in Figure A1.

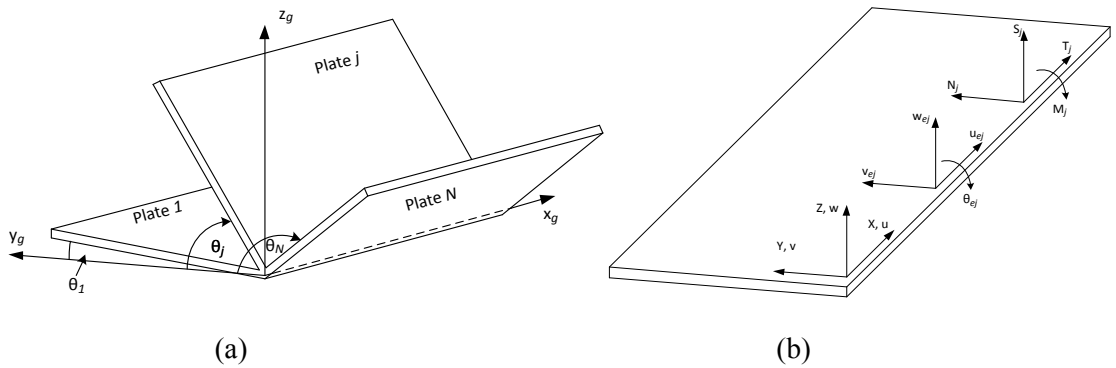

(a) (b)

Figure A1. (a) Schematic of plate/plate junction with global axes, (b) Co-ordinate system, displacements and tractions for plate *j* (as used in Ref. [6]).

The principal equation in SEA is the power balance equation between subsystems [22]. For Subsystem *j* interconnected to Subsystem *k,* with *k* varying, the power balance equation can then be written as:

$$\omega\eta_j E_j + \sum_k \omega\eta_{jk} n_j \left(\frac{E_j}{n_j} - \frac{E_k}{n_k}\right) = P_{in,j} \tag{A1}$$

where ω is the vibration frequency (rad/s), η_j is the loss factor of Subsystem *j*, η_{jk} is the coupling loss factor from Subsystem *j* to Subsystem *k*, E_j is the energy of Subsystem *j*, n_j is the modal density of Subsystem *j*, and $P_{in,j}$ is the external input power to subsystem *j*. Equation (A1) can be written in matrix form:

$$\mathbf{C}\hat{\mathbf{E}} = \mathbf{P}_{\text{in}} \tag{A2}$$

where:

$$\mathbf{C} = \omega \begin{pmatrix} \left(\eta_1 + \sum_{j=1, j\neq k}^{k} \eta_{1j}\right) n_1 & -\eta_{12} n_1 & \cdots & -\eta_{1k} n_1 \\ -\eta_{21} n_2 & \left(\eta_2 + \sum_{j=1, j\neq k}^{k} \eta_{2j}\right) n_2 & \ddots & -\eta_{2k} n_2 \\ \vdots & \ddots & \ddots & \vdots \\ -\eta_{k1} n_k & -\eta_{k2} n_k & \cdots & \left(\eta_k + \sum_{j=1, j\neq k}^{k} \eta_{kj}\right) n_k \end{pmatrix} \tag{A3}$$

and where $\hat{\mathbf{E}} = (\hat{E}_1 \quad \hat{E}_2 \quad \cdots \quad \hat{E}_k)^{\mathrm{T}}$ is the modal energy matrix, with $\hat{E}_k = E_k/n_k$ being the modal energy of Subsystem *k*, and $\mathbf{P}_{in} = (P_{in,1} \quad P_{in,2} \quad \cdots \quad P_{in,k})^{\mathrm{T}}$ is the external power input vector. To compute the required mean of the spatially-averaged structural response energy for equation (8), the parameters required by SEA for use in equation (A2), are explained in [22], namely: i) the Coupling Loss Factors (in terms of Transmission Coefficients), ii) the Modal Density, and iii) the Power Input. To correctly calculate the variance of the response energy, evaluation of the SEA parameters are made specific here to an L-shaped plate structure. The explicit variance equations are thus highlighted. Obtaining these SEA parameters is now summarised.

The Coupling Loss Factors

The coupling loss factors needed in Equation (A2) are a function of the transmission coefficient. For a line connection, as explained in [6], this can be written as:

$$\langle \eta_{pr}^{ij}(\omega) \rangle = \frac{c_{pi} L \langle \tau_{pr}^{ij}(\omega) \rangle}{\pi \omega \mathrm{A}_i} \tag{A4}$$

where $\langle \eta_{pr}^{ij}(\omega) \rangle$ represents the average coupling loss factor between wave type p of Plate i, and wave type r of Plate j, c_{pi} is the appropriate group speed of Plate i, A_i is the area of Plate i, L is the length of the junction, and $\langle \tau_{pr}^{ij}(\omega) \rangle$ represents the average transmission coefficient.

The Transmission Coefficients

The transmission coefficients needed in equation (A4) are the most important parameters for SEA. Computation of the transmission coefficients associated with an L-shaped plate structure with a line junction, can be adapted from the general approach given in [6] for a built-up structure comprising N semi-infinite, obliquely-angled plates, coupled at one line junction as shown in figure A1a. The method in [6] is based on a wave approach including bending, longitudinal, and shear waves, where in figure 1a, θ_1, θ_j, and θ_N are the angles between the global *y* axis and Plate-1, Plate-*j*, and Plate-*N*, respectively. The co-ordinate system, displacements, and tractions for Plate- j, are shown in Figure A1b. By choosing N = 2 and respectively setting $\theta_1 = 0$ and $\theta_2 = \pi/2$ allows the theory to be adapted. Starting from the fundamental plate equation with bending, longitudinal, and shear waves, the dynamic stiffness matrix is constructed in [6] for Plate-*j* both with, and without incident waves. When an incident wave is not carried by Plate-*j*, the theory gives a relationship between the vector of displacements $\mathbf{b}_j = (u_{ej}\ v_{ej}\ w_{ej}\ \theta_{ej})^{\mathrm{T}}$ and the vector of tractions $\mathbf{F}_j = (T_j\ N_j\ S_j\ M_j)^{\mathrm{T}}$ i.e.:

$$\mathbf{F}_j = \mathbf{K}_j \mathbf{b}_j \tag{A5}$$

where $\mathbf{K}_j$ is the dynamic stiffness matrix, with elements given explicitly in [6]: An appropriate modification to equation (A5) applies when an incident wave is carried by Plate-*j*. The edge displacement vector $\mathbf{b}_j$ can be calculated and used to solve for the response wave amplitudes ($\alpha_{B1},\ \alpha_{B2}, \alpha_L, \alpha_S$) of Plate-*j.* The amplitudes can in turn be used to compute the input power terms: $P_B,\ P_L$, and $P_S,$ for the three types of wave. The transmission coefficient associated with each of the generated waves can then be calculated by taking the ratio of the transmitted power to the total power, for waves incident to the junction. The transmission coefficient for the complete set can be written in the form $\tau_{pr}^{ij}(\omega, \phi)$, where $i,\ p,\ \omega$ and ϕ are the carrier plate, wave type, frequency, and heading of the incident wave, and j and r are the carrier plate and wave type of a generated wave. For $i = j$, τ is known as a refection coefficient. The conservation of energy requires that:

$$\sum_r \sum_j \tau_{pr}^{ij}(\omega, \phi) = 1 \tag{A6}$$

Finally, the average transmission coefficient is obtained as follows:

$$\langle \tau_{pr}^{ij}(\omega) \rangle = \frac{1}{2} \int_0^{\pi} \tau_{pr}^{ij}(\omega, \phi) \sin\phi \, d\phi \tag{A7}$$

The Modal Density

The modal density (mode/rad) for a plate, as needed in equation (A1), is given in [22] as:

$$n_r(\omega) = \frac{\mathrm{A}{k_r}^2}{4\pi c_{\phi r}} \tag{A8}$$

where n_r, k_r, and $c_{\phi r}$ are respectively the modal density, wave number, and phase speed for a wave type r, and *A* is the area of a plate. The wave number for each wave type is given in [6] where the phase speed is defined as $c_{\phi r} = \omega / k_r$.

The power input

The input power needed in equation (A2) can, from Ref [22], be written:

$$P_{in} = \frac{|F|^2 Re\{Y(\omega)\}}{2} \tag{A9}$$

where $|F|$ is the force amplitude, and $Re\{Y(\omega)\}$ is the real part of the point mobility. For an infinite plate $Y(\omega) = 1/(8\sqrt{D\rho})$ [32], and the power input for a unit point force is:

$$P_{in}^{\infty} = \frac{1}{16\sqrt{D\rho}} \tag{A10}$$

The Variance of the Energy

Prediction of the variance of the energy response has been difficult for SEA. The most accurate method for built-up structures is given in [24]. The energy variance can be written in the form:

$$\mathrm{Var}\left[\hat{E}_j\right] = \sum_k \left(D_{0,jk}^{-1}\right)^2 \mathrm{Var}\left[P_{\mathrm{ran},k}\right] + \sum_k \sum_{s \neq k} \left[\left(D_{0,jk}^{-1} - D_{0,js}^{-1}\right)\hat{E}_s\right]^2 \mathrm{Var}\left[D_{\mathrm{ran},ks}\right] \tag{A11}$$

where $D_{0,jk}^{-1}$ represents the jk entry of the matrix $\mathbf{D}_0^{-1}$, the inverse of the SEA matrix $\mathbf{C}$ in equation (A2), $\hat{E}_s$ is the ensemble averaged modal energy obtained by SEA. The input power variance $\mathrm{Var}\left[P_{\mathrm{ran},k}\right]$ is given in detail in [24].

These summarised SEA results for an L-shaped plate are applied in order to compare with Direct Integration of Section 2. To verify implementation of these SEA methods, a replication check is shown in Figure 3 as compared with results for obliquely coupled-plates published in [24].

References

[1] G. Manson, Calculating frequency response functions for uncertain systems using complex affine analysis, Journal of Sound and Vibration 288 (3) (2005) 487–521.

[2] S. Donders, D. Vandepitte, J. Van de Peer, W. Desmet, Assessment of uncertainty on structural dynamic responses with The Short Transformation method, Journal of Sound and Vibration 288 (2005) 523–549.

[3] D. Moens, M. Hanss, Non-probabilistic finite element analysis for parametric uncertainty treatment in applied mechanics: Recent advances, Finite Elements in Analysis and Design 47 (1) (2011) 4–16.

[4] H. De Gersem, D. Moens, W. Desmet, D. Vandepitte, A fuzzy finite element procedure for the calculation of uncertain frequency response functions of damped structures: Part 2—Numerical case studies, Journal of Sound and Vibration, 288 (3) (2005) 463-486.

[5] M. A. Valdebenito, H. A. Jensen, M. Beer, C. A. Perez, Approximate Fuzzy Structural Analysis Applying Taylor Series and Intervening Variables, 10th World Congress on Structural and Multidisciplinary Optimization May 19 – 24 (2013) Orlando, Florida, USA.

[6] R. Langley, K. Heron, Elastic wave transmission through plate/beam junctions, Journal of Sound and Vibration 143 (1990) 241-253.

[7] C. Manohar, R. Ibrahim, Progress in structural dynamics with stochastic parameter variation: 1987-1998, Applied Mechanics Reviews 52 (5) (1999) 177-197.

[8] R. Langley, Unified approach to probabilistic and possibilistic analysis of uncertain systems, Journal of Engineering Mechanics 126 (11) (2000) 1163-1172.

[9] B. Mace, Preface—uncertainty in dynamics, Journal of Sound and Vibration 288 (2005) 423–429.

[10] H. Pradlwarter, G Schueller, A Consistent Concept for High and Low Frequency Dynamics Based on Stochastic Modal Analysis, Journal of Sound and Vibration 288 (3) (2005) 653–667.

[11] P.J. Shorter, R.S. Langley, Vibro-acoustic analysis of complex systems., Journal of Sound and Vibration 288 (2005) 669 – 699.

[12] L. W. Dunne, J. F. Dunne, An FRF Bounding Method for Randomly Uncertain Structures with or without Coupling to an Acoustic Cavity, Journal of Sound and Vibration 322 (2009), 98–134

[13] G. Guoqing, J.F. Dunne, Efficient exceedance probability computation for randomly uncertain nonlinear structures with periodic loading, Journal of Sound and Vibration 330 (2011) 2354–2368.

[14] H. Benaroya, M. Rehak, Finite element methods in probabilistic structural analysis: A selective review, Applied Mechanics Reviews 41 (5) (1988) 201-213.

[15] K. Breitung, L. Faravelli, Response surface methods and asymptotic approximations, Mathematical Models for Structural Reliability Analysis (1996) CRC Press, Boca Raton.

[16] R. Langley, The dynamic analysis of uncertain structures (Plenary Paper). The Seventh International Conference on Recent Advances in Structural Dynamics, ISVR, Southampton, (2000).

[17] H. Madsen, S. Krenk, N. Lind, Methods of Structural Safety, (2006) Dover Publications.

[18] R. Melchers, M. Ahammed, C. Middleton, FORM for discontinuous and truncated probability density functions, Structural Safety 25 (3) (2003) 305–313.

[19] E. Patelli, H.J. Pradlwarter, G. I. Schueller, On multinormal integrals by importance sampling for parallel system reliability**,** Structural Safety 33 (1) (2011) 1-7.

[20] H. J. Pradlwarter, G. Schueller, P. S. Koutsourelakis, D. C. Charmpis, Application of line sampling simulation method to reliability benchmark problems, Structural Safety 29 (3) (2007) 208-221.

[21] G. I. Schueller, H. J. Pradlwarter Computational Stochastic Structural Analysis (COSSAN) – a software tool, *Structural Safety* 28 (1-2) (2006) 68 – 82.

[22] R. Lyon, R. de Jong Theory and Application of Statistical Energy Analysis, 2nd edition, (1995) Butterworth-Heinemann.

[23] C. Burroughs, R. Fischer, F. Kern, An Introduction to Statistical Energy Analysis, Journal of the Acoustical Society of America, 101 (4) (1997) 1779-1789.

[24] R. Langley, V. Cotoni Response variance prediction in the statistical energy analysis of built-up systems, Journal of the Acoustical Society of America 115 (2004) 706-718.

[25] V. Cotoni, R. Langley, M. Kinder, Numerical and experimental validation of variance prediction in the statistical energy analysis of built-up systems, Journal of Sound and Vibration 288 (3) (2005) 701-728.

[26] A. Le Bot, V. Cotoni, Validity diagrams of statistical energy analysis, Journal of Sound and Vibration 329 (2010) 221-235.

[27] A. Cicirello, R. Langley, Efficient parametric uncertainty analysis within the hybrid Finite Element/Statistical Energy Analysis method, Journal of Sound and Vibration 333 (6) (2014) 1698–1717.

[28] A. Secgin, J. Dunne, L. Zoghaib, Extreme-Value-Based Statistical Bounding of Low, Mid, and High Frequency Responses of a Forced Plate with Random Boundary Conditions, ASME Journal of Vibration and Acoustics 134 (2012).

[29] R. Langley, J. Legault, J. Woodhouse, E. Reynders On the applicability of the lognormal distribution in random dynamical systems, Journal of Sound and Vibration 332 (2013) 3289-3302.

[30] S. Coles, An Introduction to Statistical Modelling of Extreme-Values, (2001) Springer, London.

[31] N. L. Johnson, S. Kotz, N. Balakrishnan, Continuous Univariate Distributions, (1994) Vol. 1, 2nd Edition, Wiley Interscience. (p207 -220).

[32] L. Cremer, M. Heckl, B. Petersson, Structure borne sound (1973) Springer-Verlag.

Figure Captions

Figure 1. An L-shaped plate showing the location of a point-force harmonic excitation on Plate-1.

Figure 2. The energy of Plates 1 and 2 as functions of the plate thickness with 150 subintervals at frequencies 5005 Hz and 10000 Hz, for an L-shaped plate subjected to a single harmonic load on Plate 1.

Figure 3. The mean and relative variance of the energy of Plates 1 and 2 versus frequency, for two coupled plates with a harmonic point loading on Plate 1: (a) reproduced result, (b) taken from Fig. 3 of Ref [26].

Figure 4. The predicted mean of the energy of Plate 1, for an L-shaped plate with dimension variability: • FE Monte Carlo simulation; − DI; **---** SEA.

Figure 5. The predicted standard deviation of the energy of Plate 1, for an L-shaped plate with dimension variability: • FE Monte Carlo simulation; − DI; **---** SEA.

Figure 6. The predicted mean of the energy of Plate 1, for an L-shaped plate with thickness variability: • FE Monte Carlo simulation; − DI; **---** SEA.

Figure 7. The predicted standard deviation of the energy of Plate 1, for an L-shaped plate with thickness variability: • FE Monte Carlo simulation; − DI; **---** SEA.

Figure 8. The energy response bounds for Plate 1 in terms of the 50%-quantile associated with the extreme value distribution for an L-shaped plate with dimension variability: − DI; **---** SEA, showing the FRF for 100 realised structures (grey).

Figure 9. The energy response bounds for Plate 1 in terms of the 50%-quantile associated with the extreme value distribution for an L-shaped plate with thickness variability: − DI; **---** SEA, showing the FRF for 100 realised structures (grey).

LIST OF FIGURES

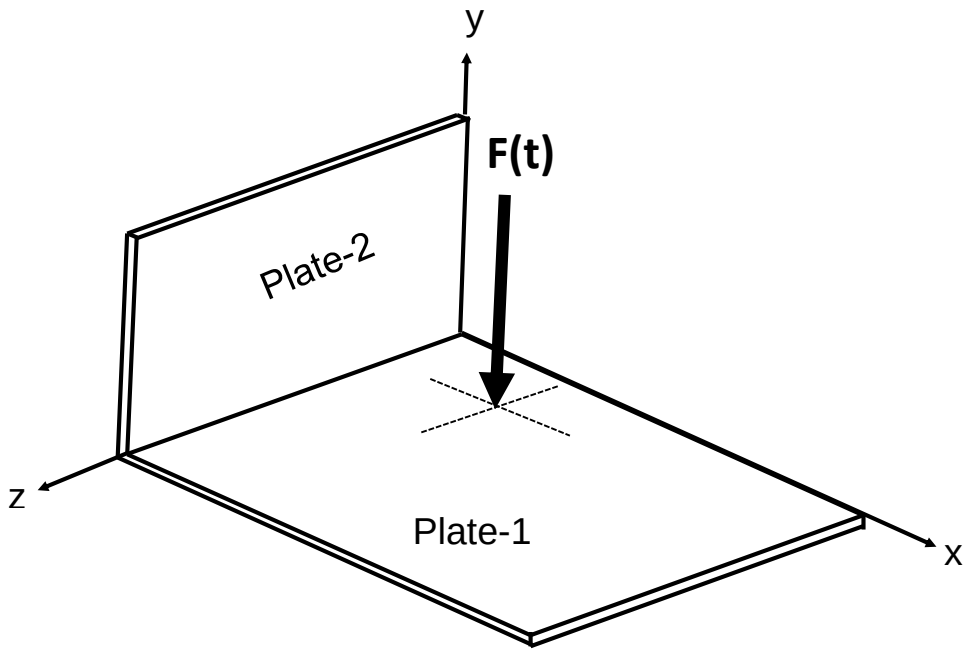

Figure 1. An L-shaped plate showing the location of a point-force harmonic excitation on Plate-1.

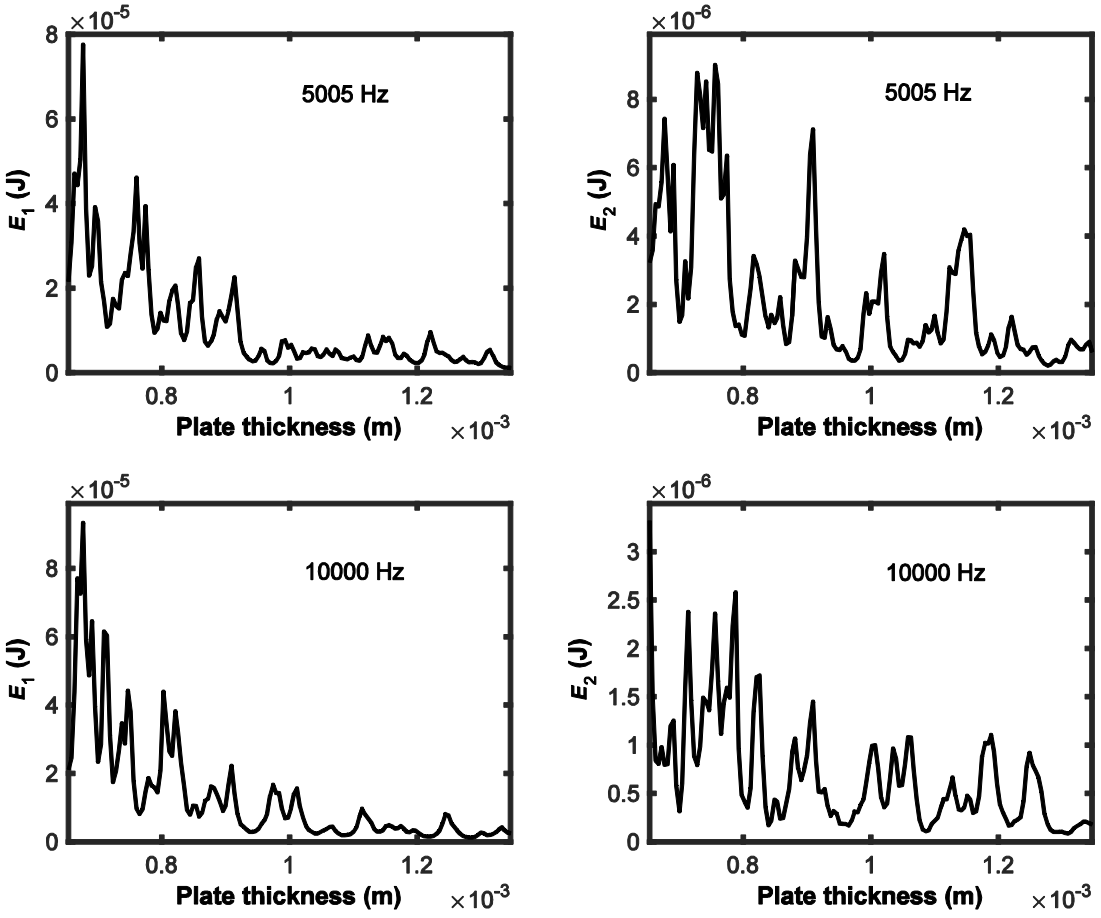

Figure 2. The energy of Plates 1 and 2 as functions of plate thickness with 150 subintervals at frequencies 5005 Hz and 10000 Hz, for an L-shaped plate subjected to a single harmonic load on Plate 1.

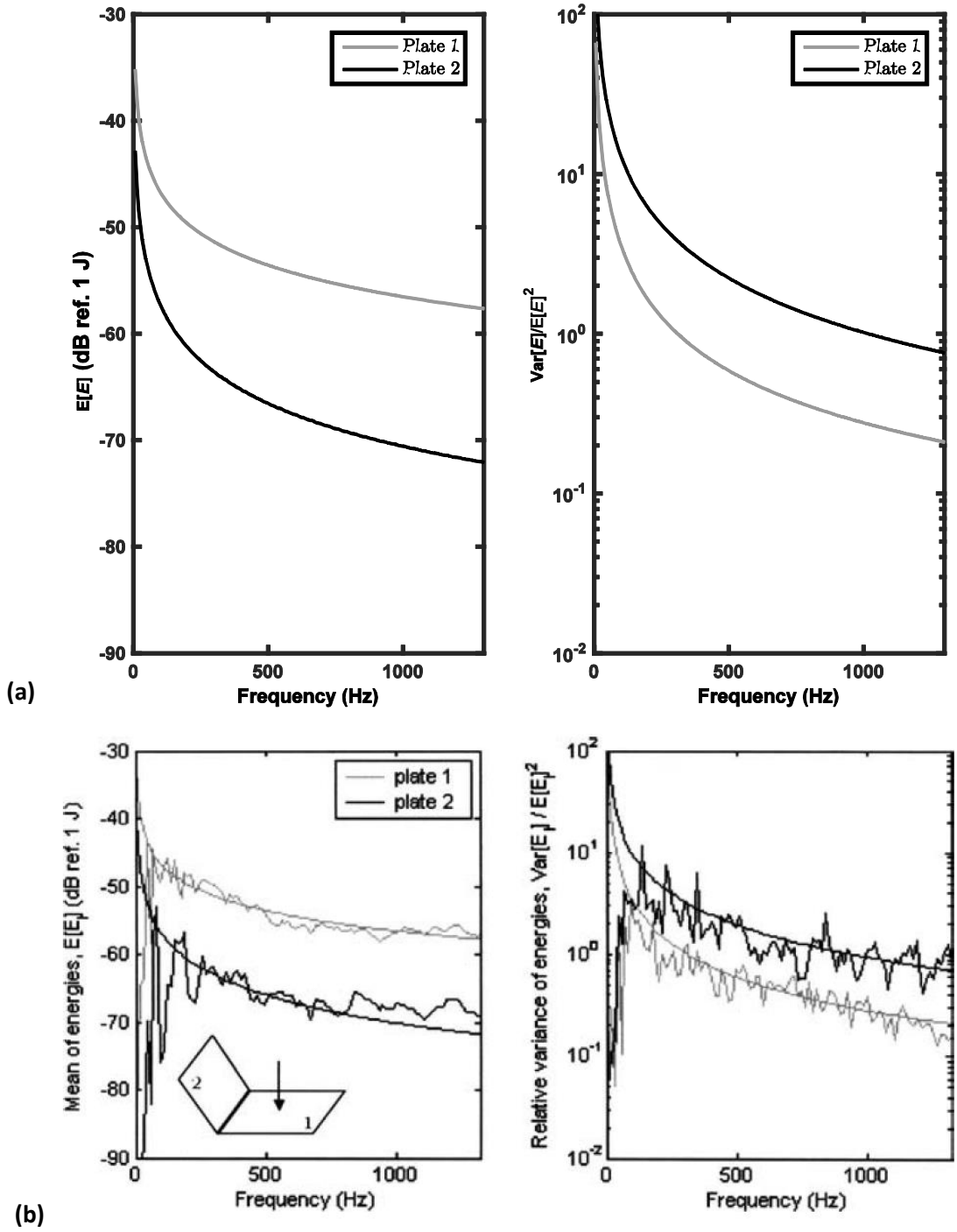

Figure 3. The mean and relative variance of the energy of Plates 1 and 2 versus frequency, for two coupled plates with a harmonic point loading on Plate 1: (a) reproduced result, (b) taken from Fig. 3 of Ref [24].

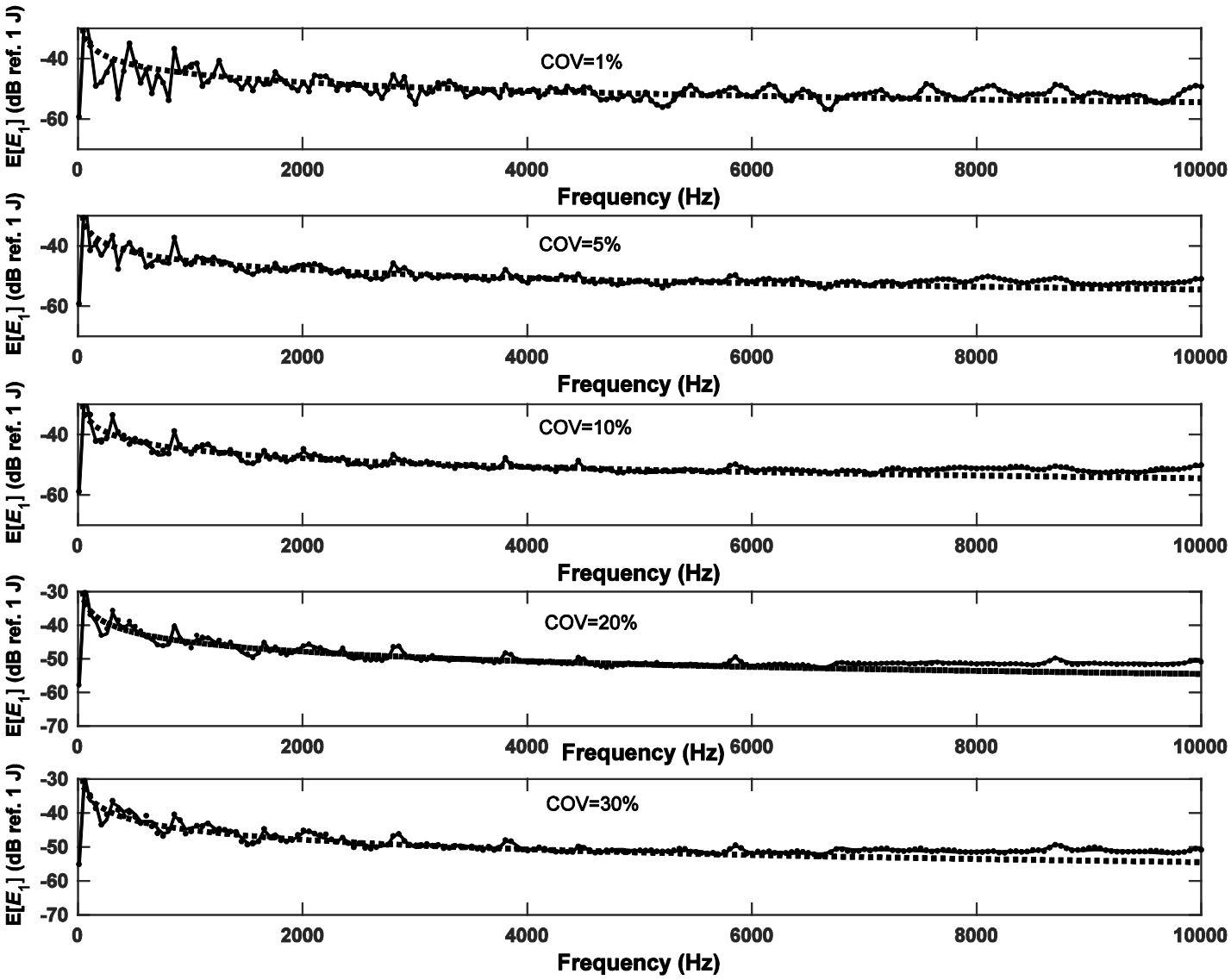

Figure 4. The predicted mean of the energy of Plate 1, for an L-shaped plate with dimension variability: • FE Monte Carlo simulation; − DI; --- SEA.

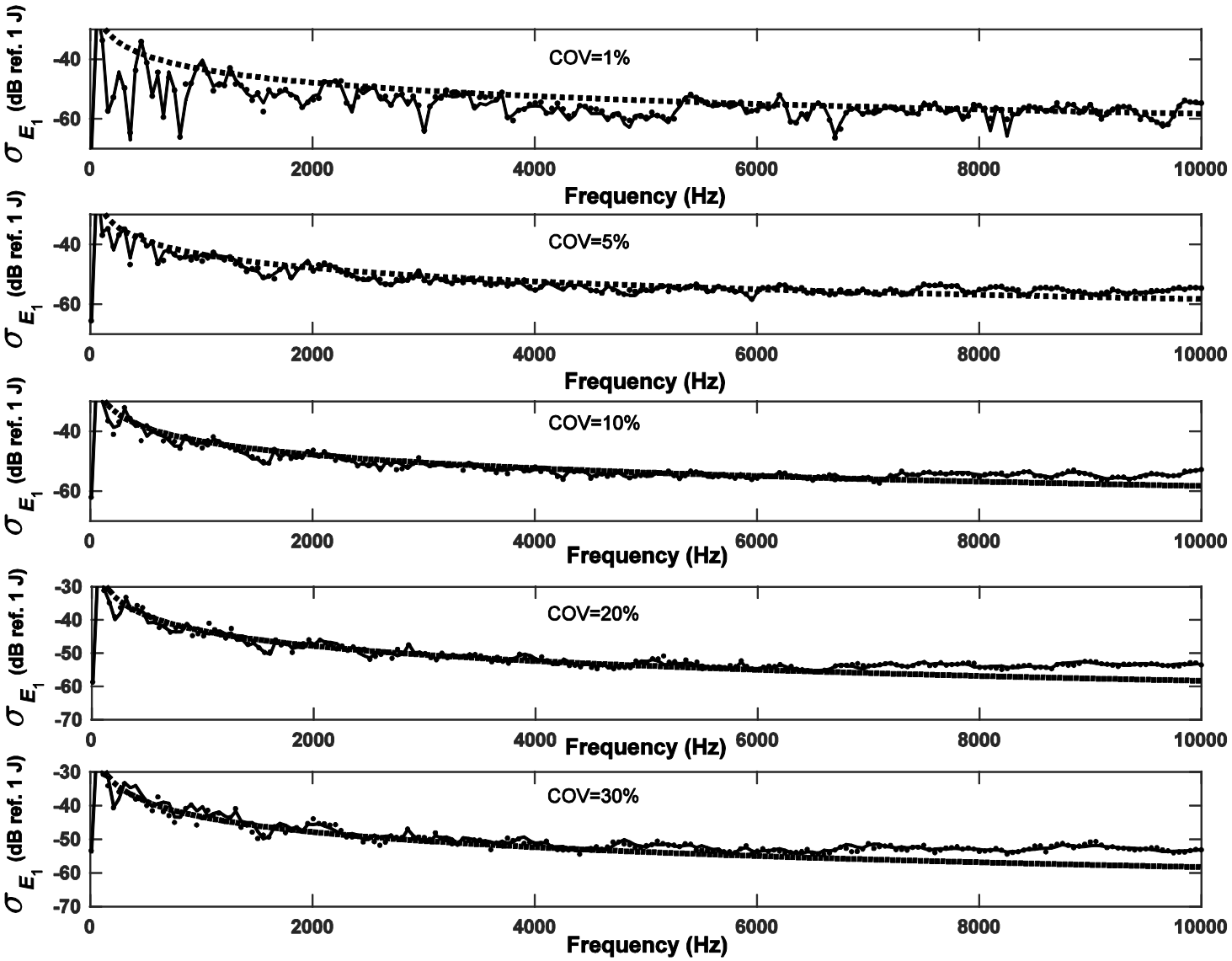

Figure 5. The predicted standard deviation of the energy of Plate 1, for an L-shaped plate with dimension variability: • FE Monte Carlo simulation; − DI; --- SEA.

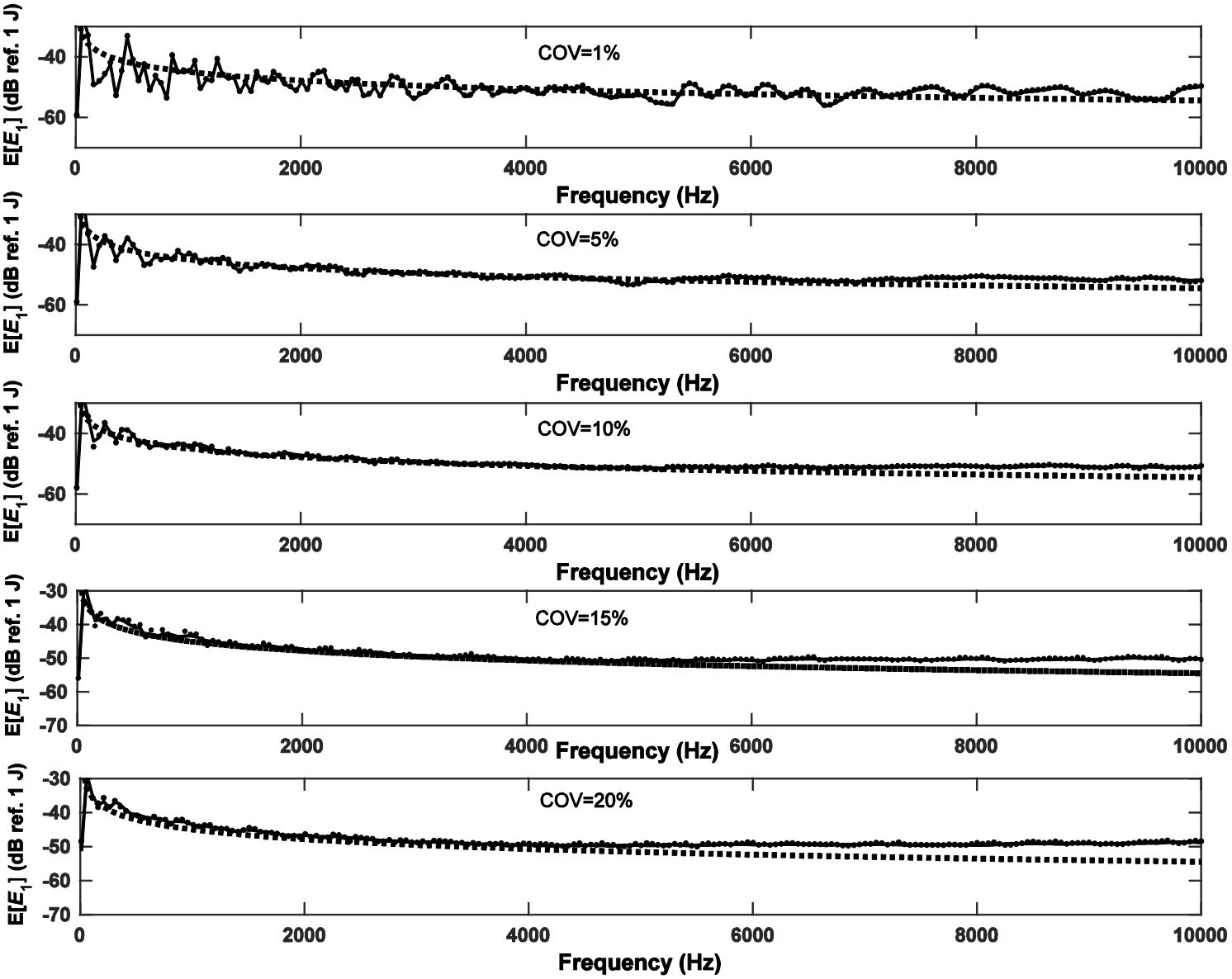

Figure 6. The predicted mean of the energy of Plate 1, for an L-shaped plate with thickness variability: • FE Monte Carlo simulation; − DI; --- SEA.

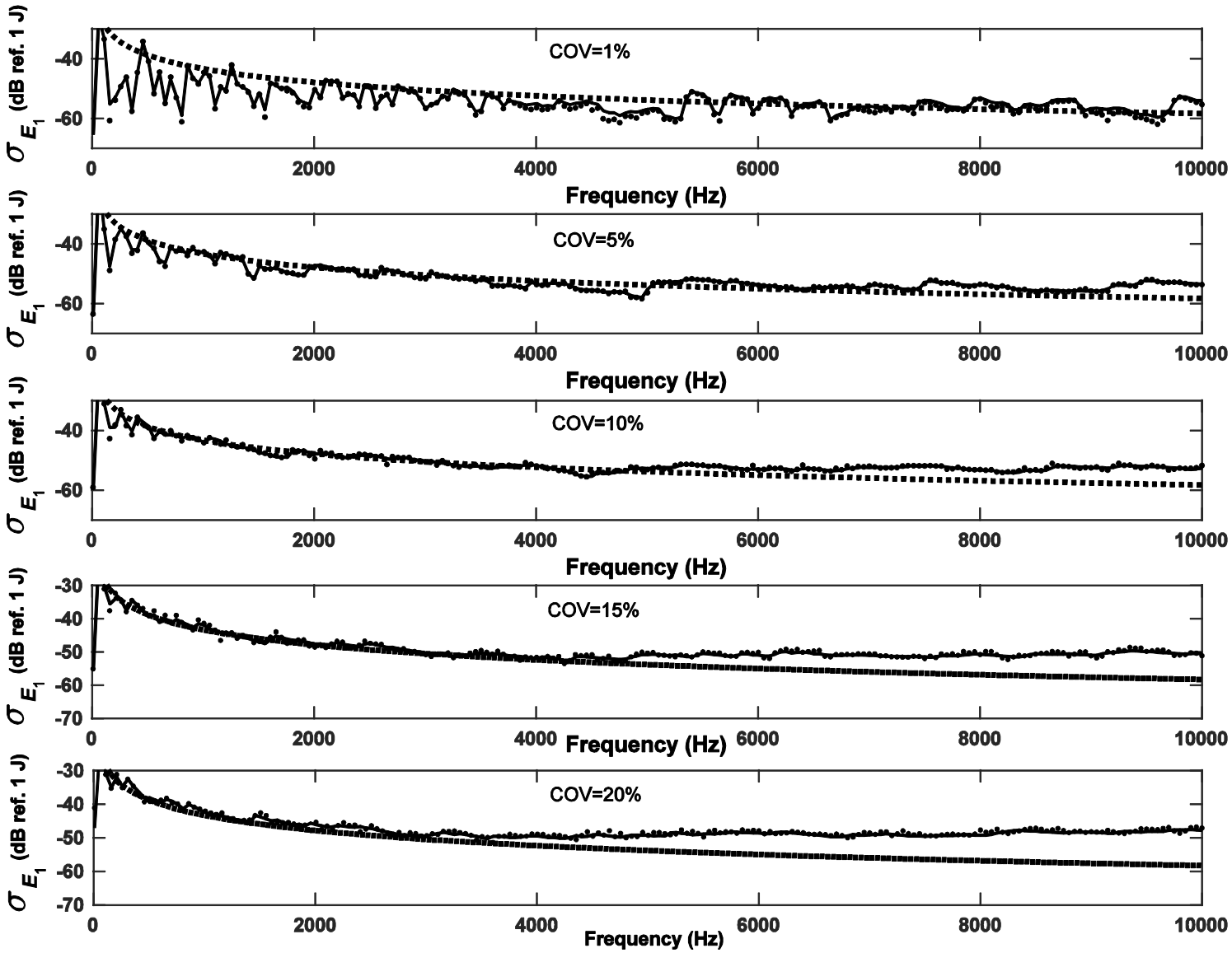

Figure 7. The predicted standard deviation of the energy of Plate 1, for an L-shaped plate with thickness variability: • FE Monte Carlo simulation; − DI; --- SEA.

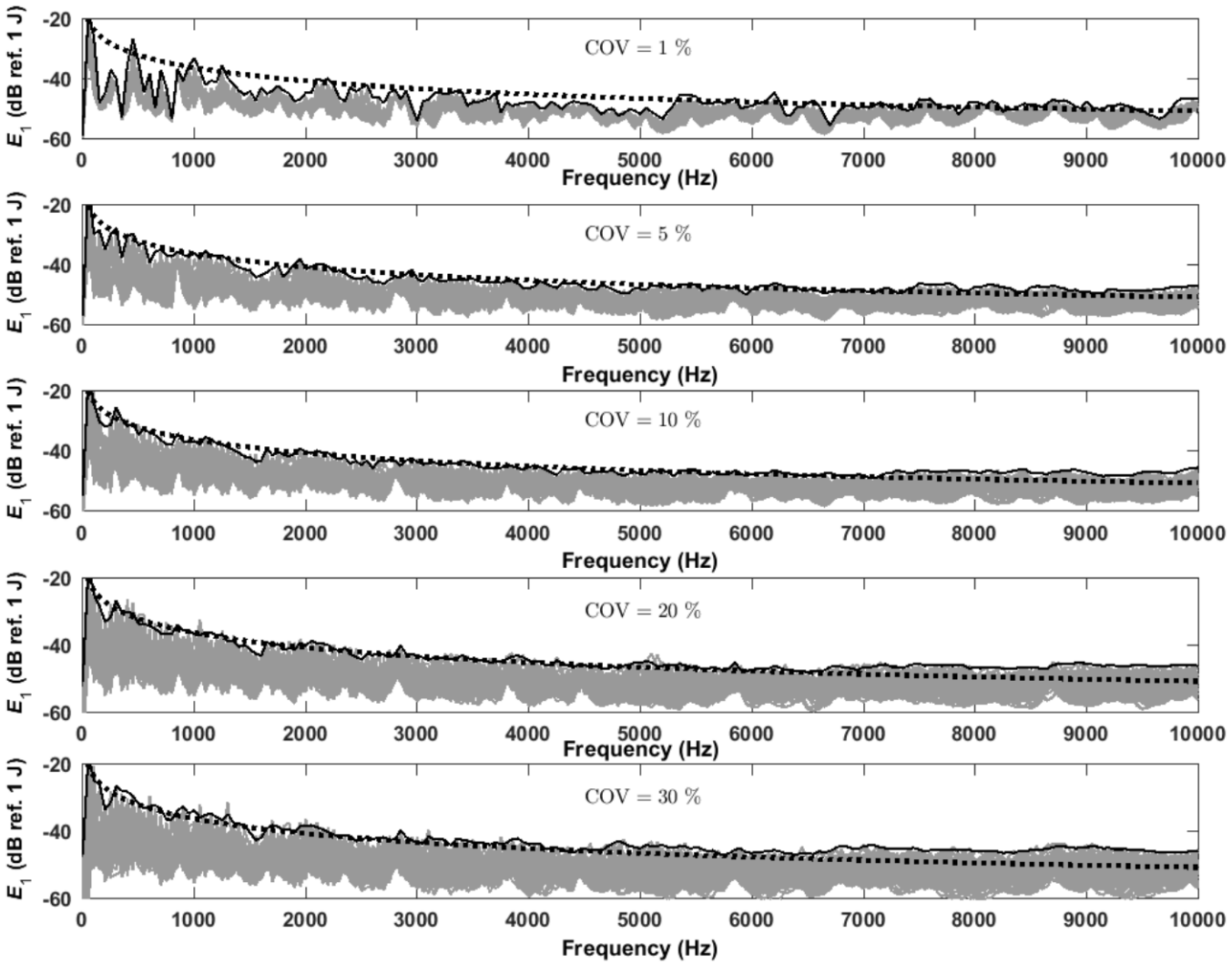

Figure 8. The energy response bounds for Plate 1 in terms of the 50%-quantile associated with the extreme value distribution for an L-shaped plate with dimension variability: − DI; --- SEA, showing the FRF for 100 realised structures (grey).

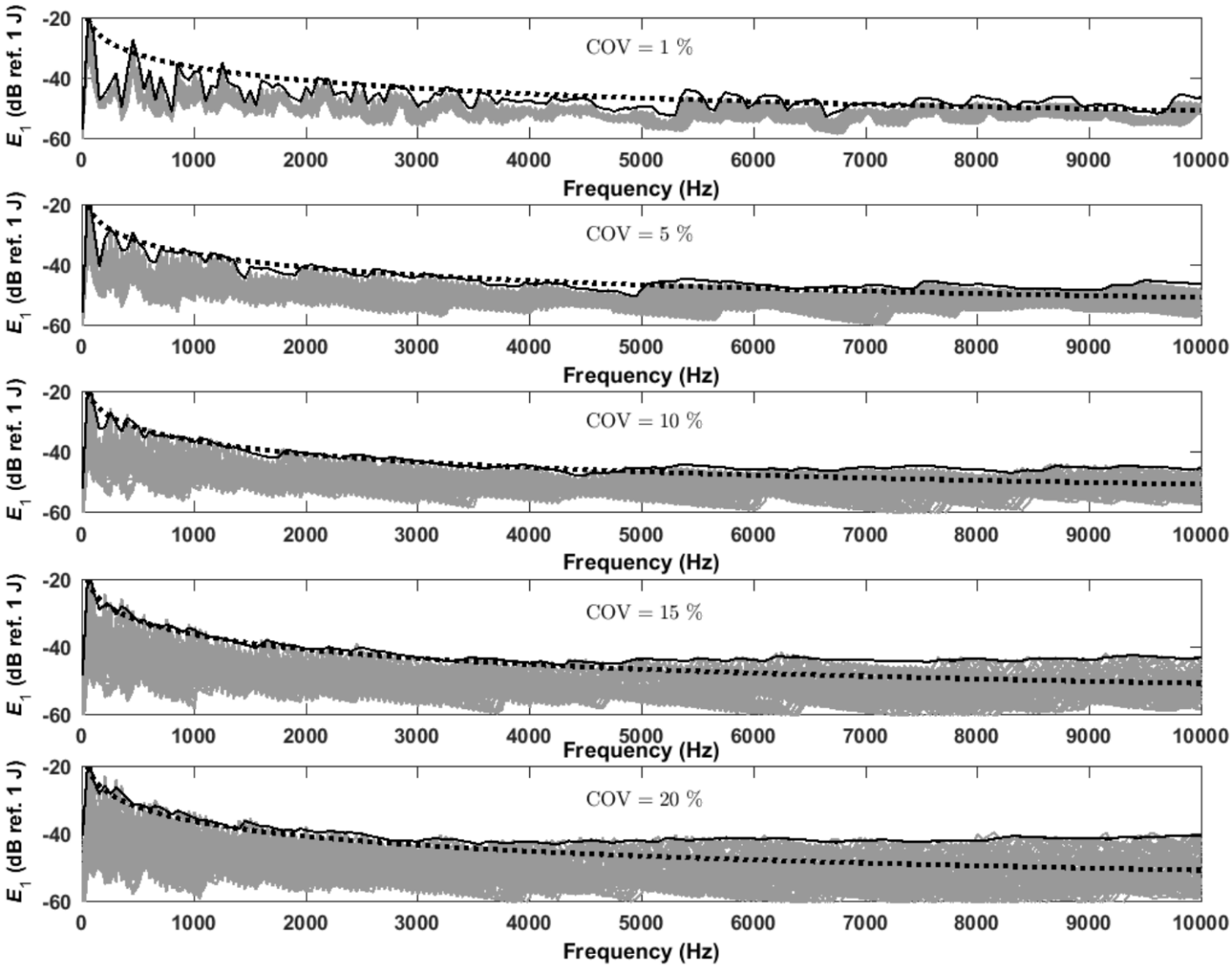

Figure 9. The energy response bounds for Plate 1 in terms of the 50%-quantile associated with the extreme value distribution for an L-shaped plate with thickness variability: − DI; --- SEA, showing the FRF for 100 realised structures (grey).